

Electronic Shell Structure of Group-III A Metal Atomic Clusters

Kenneth E. Schriver, John L. Persson,^(a) Eric C. Honea,^(a) and Robert L. Whetten

Department of Chemistry and Biochemistry and Solid State Science Center, University of California,
Los Angeles, California 90024-1569

(Received 20 October 1989)

Ionization potentials of Al_n and In_n clusters ($n < 80$) in supercooled beams have been measured by photoionization spectroscopy. The abrupt leveling near $n=5$ of the initial linear increase in ionization potentials and the subsequent gradual approach to the classical metallic sphere model are consistent with a simple picture of s - p band hybridization. For $n > 6$, there is clear evidence of electron shell filling, yet substantial deviations from shell-model predictions remain. Crystal-field effects are considered the most probable source of symmetry breaking and give insight to cluster structure.

PACS numbers: 71.50.+t, 36.40.+d

The discovery of the electronic shell structure¹ in the alkali-metal atomic clusters K_n and Na_n has stimulated renewed interest in the electronic properties of very small metal particles.² Because the observed shell-filling numbers are predicted by a spherical jellium background model (SJBM),³ or its spheroidal variant,⁴ one expects that the properties of all free-electron metal clusters might be unified within this simple model.⁵ Jellium-based calculations also predict a set of shell-filling numbers for divalent and trivalent atomic clusters.⁶ However, small clusters of the group-II metals Ba and Hg seem to exhibit insulator band structure; a gradual transition to metallic bands occurs over the $n=20$ -60 region (Hg) (Refs. 7 and 8) or beyond 30 (Ba),⁹ without evident shell structure. Particularly revealing are ionization-energy patterns which deviate systematically from the classical electrostatic law,¹⁰ which had been found to hold very well for the alkali metals.²

For group-III metals, *ab initio* calculations on Al_n clusters ($n < 14$) indicate a gap between bands derived from the $3s$ and $3p$ atomic orbitals,¹¹ whereas macroscopic (fcc) Al is well described by the nearly-free-electron model, in which deviations from free-electron energy levels occur only near Brillouin-zone boundaries. Electronic properties of larger clusters should correspondingly be free-electron-like, as in the jellium model, with symmetry-specific deviations arising from particular lattice structures.¹¹ Experimentally, partial confirmation of shell-model predictions for Al_n in the $n=7$ -30 range has been deduced from photoelectron spectra,^{12,13} ionization potentials,¹⁴ and binding energies.¹⁵ However, in this Letter, we present photoionization-spectroscopic results on the electronic properties of Al_n and In_n clusters, $n < 80$, which show a nonclassical IP evolution, exposing the full range of an s - p hybridization transition, as well as very specific deviations from the SJBM throughout, implicating significant symmetry breaking.

The atomic cluster beams are produced by laser vaporization of the corresponding metal rod, and are carried in a supersonic gas jet formed by pulsing high-pressure He

(ca. 7 atm) over the rod. The gas pulse expands into vacuum through a Laval-type nozzle optimized for cluster growth and cooling. The cooling is sufficient that species such as Al_nAr_m are formed from the condensation of Ar added to the He gas.¹⁶ Photoionization is by fixed-energy (7.87 or 6.42 eV) or tunable (frequency-doubled dye laser, 5-6 eV) ultraviolet radiation with the cluster ions mass analyzed by time-of-flight mass spectrometry. Ionization thresholds are measured at fluences below 10^{-4} J/cm², where the signal intensity depends linearly on ionization-laser fluence. Further details on the apparatus and procedure used are given in Ref. 16. Figure 1 shows the photoionization-threshold-energy (IP) pattern for Al_n as a function of n (number of atoms) and $n_e = 3n$ (number of electrons). These values are obtained from analysis of photoionization spectra,

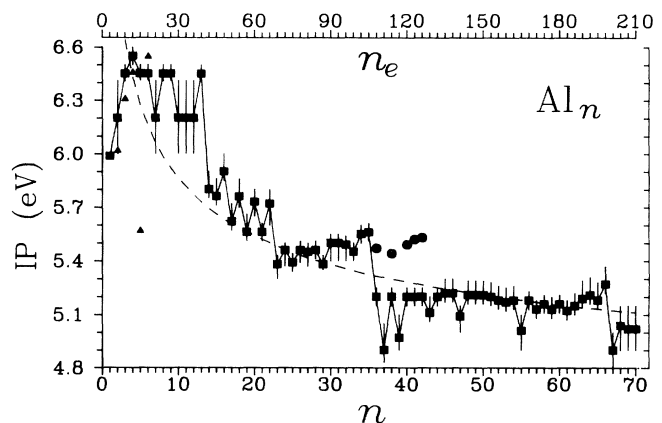


FIG. 1. Ionization threshold energies (IP) of Al_n clusters plotted as a function of n . Data points in the $n=3$ -8 region and upper bounds on $n=9$ -13 are taken from Ref. 14. The filled triangles are from Upton's *ab initio* computations (Ref. 11), and the dashed curve is the classical metallic sphere model (Ref. 10), $\phi + \frac{3}{8} e^2/R$, using the bulk density and work function ($\phi=4.28$ eV). Circles in the $n=36$ -42 region represent above-threshold photoionization spectral features.

acquired as continuous scans in the 5.5–5.9-eV region, and from 0.05-eV interval data below 5.5 eV. Threshold energies are assigned to the base-line intercept of the best straight line through the final decline of the photoionization spectrum. In_n-cluster IP's are bounded from a series of photoionization mass spectra in the 5.2–6.4-eV region.

The ionization potential of Al_n clusters (Fig. 1) increases steeply at small *n*, and threshold ionization energies for *n*=3–6, 8, 9, and 13 are all 0.5 eV or more above the atomic value. A very large decrease from *n*=13 to 14 is followed by a general decline that gradually approaches the classical metallic sphere model.¹⁰ [Our observations are consistent with Cox *et al.*,¹⁴ except that Al₉ and Al₁₃ data are now interpreted such that IP > 6.4 eV, Fig. 3(a).] In the case of In_n, it is similarly found that *n*=2–6, 8, and 9 have IP's at least 0.25 eV above the atomic value.

The IP trend for Al_n, *n*=2–6, has been explained by Upton¹¹ in terms of delocalized bonding orbitals derived from atomic 3*p* orbitals, though his calculated drop in the IP at *n*=5 is not observed. Both this initial rise and the sustained high ionization potentials (Fig. 1) represent substantial deviations from the classical trend followed by alkali-metal atomic clusters.¹⁰ A proposal for understanding the differences among the group-I, -II, and -III atomic clusters is related to the insulator-metal transitions known for expanded metals, such as near-critical Hg vapor.¹⁷ This picture,^{7,11} illustrated in Fig. 2, emphasizes the evolution and hybridization of the *s* and *p* bands as a function of the density or size or mean coordination number of the material system. In monovalent metals (Na, K, Cu) the *s* band is always half-filled, and theory and experiment agree on delocalized electron states for even the smallest clusters. Divalent metals differ sharply: Small clusters exhibit weak bonding and localized electrons in the filled *s* bands until undergoing the insulator-metal transition. Group-III metals are characterized for small *n* by a one-sixth-filled *p* band, where only the deepest-lying bonding orbitals are occupied, giving rise to the initial increase in IP's. As the *s* and *p* bands hybridize, the IP's approach the classical prediction. Specifically for Al_n, we suggest that the abrupt leveling of the initial linear increase in IP's at *n*=5 atoms indicates the onset of *s-p* hybridization. The continued hybridization is manifested in the sustained high IP's of *n*=5–22 atoms, and only when the IP's merge with the classical curve in the *n*=25–45 range (where the exact size for merging depends on how the shell structure is interpreted) is the hybridization completed (Fig. 1). Some direct evidence for an onset of the

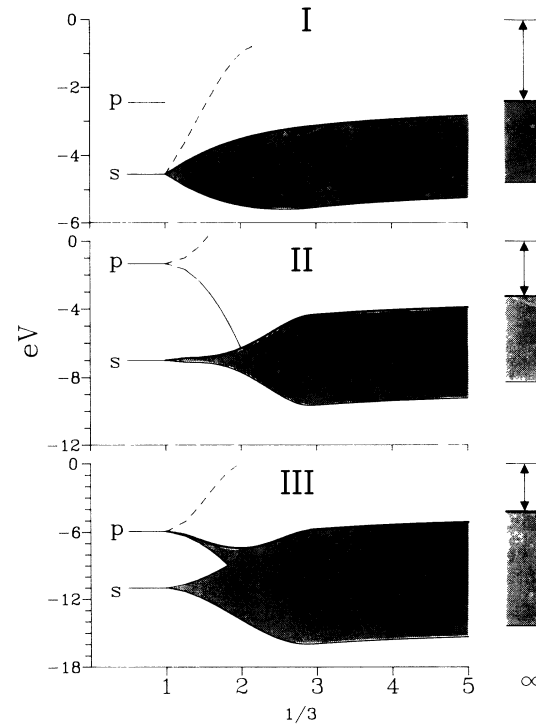


FIG. 2. Hypothetical size evolution of the electron bands of clusters composed of *n* group-I (upper), -II (middle), and -III (lower) metal atoms. The *s* and *p* orbital energies of the bulk Fermi energies and the work functions are defined with respect to vacuum and are appropriate to a mid-*Z* atom (e.g., Na or K, Mg or Ca, and Al or Ga). The asymptotic behavior of the work function is taken to be $n^{-1/3}$, as already observed for Na and K (Refs. 1 and 10) and in Fig. 1.

gradual merging of *s* and *p* bands in Al_n might also be derived from photoemission spectra,¹³ which show a steadily growing density of states at 2–4 eV below the Fermi level for *n*=18–32 atoms.

Figures 1 and 3 reveal a pronounced shell structure in Al_n clusters for *n* > 6. A shell opening at size *n* is characterized by a particularly low IP and thus a strong signal in the mass spectra (Fig. 3). The IP gradually increases with *n* as the electrons fill the shell, to reach a maximum at shell closing, and then drop discontinuously as the next shell opens.³ The discontinuities in IP for group-III metals are typically 0.2–0.6 eV, about 4 times larger than for the alkali metals.¹ The spherical shell model of Knight *et al.*¹ proposes a universal pattern of shell-filling electron numbers, while the SJBM^{2,3,6} provides quantitative predictions for the magnitude of shell effects, including gaps between shells. In this model, $n_e = nZ_A$ electrons fill the spherical orbitals $|nl\rangle$ of an *A_n* cluster according to the pattern¹⁸

$$1s^2 1p^6 | 1d^{10} 2s^2 | 1f^{14} | 2p^6 | 1g^{18} | 2d^{10} | 1h^{22} 3s^2 | 2f^{14} 1i^{26} 3p^6 | 2g^{18} 1j^{30} 3d^{10} 4s^2 | \dots, \quad (1)$$

where the vertical bars indicate the largest shell-closing discontinuities occurring at $n_e = 8, 20, 34, 40, 58, 68, 92, 138,$ and 198 electrons. For Al_n ($Z_A = 3, n_e = 3n$) we find shell openings (low IP's) at *n*=7 atoms (21 electrons), 14 (42),

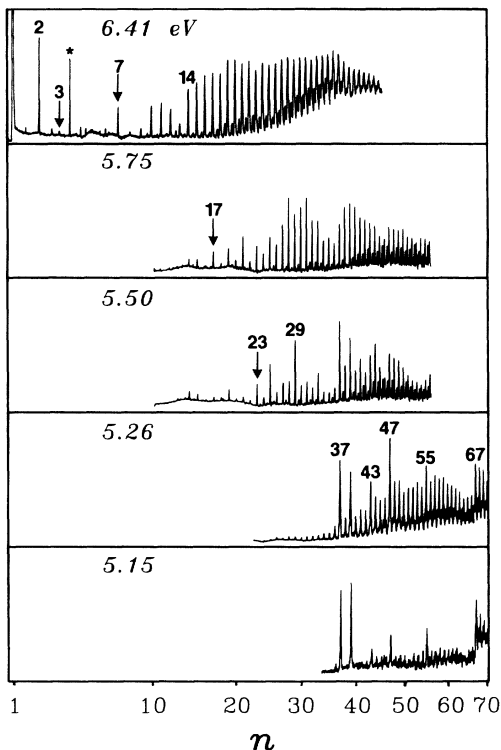


FIG. 3. Photoionization mass spectra of Al_n clusters taken at several photon energies. At 7.87-eV photoionization energy (not shown) all cluster sizes are efficiently ionized, resulting in a smooth size distribution. At lower photon energies, the mass spectra are dominated by low-IP clusters, corresponding to electron-shell openings. (The starred peak in the top frame is Al_3O .)

17 (51), 23 (69), 29 (87), 36–37 (108–111), 39 (117), 43 (129), 47 (141), 55 (165), and 67 (201). The same shell openings are found to apply to In_n (not shown), particularly $n=7, 14, 17, 37, 43,$ and 47 atoms. Using the IP information and limited data on Al_nO clusters, where $n_e = 3n - 2$, we assign the shell closings of group-III metals as $n_e = \underline{20}, \underline{40}, 50, \underline{68}, 84, 106$ or $108, 114, 126, \underline{138}, 164,$ and $\underline{198}$ electrons. The underlined shell closings show the validity of a spherical approximation with $n_e = 3n$ valence electrons, that is, a single $3s-3p$ conduction band. However, the absence of discontinuities at $n_e = 34, 58,$ and 92 electrons, together with the observed additional shell closings at $n_e = 50, 84, 106$ or $108, 114, 126,$ and 164 electrons, indicates a partial failure of the SJBM.

The range of n values studied here goes beyond previous work on Al_n clusters. Our data compare well with measured stabilities,¹⁵ but only partly with the observed electron affinities (EA): Ganteför *et al.*¹² find “outstanding high EA” for $n=4, 6, 9, 19,$ and 22 atoms and low EA for $n=14$ and 23 atoms, which, except $n=19$, is consistent with our shell picture. Taylor *et al.*¹³ find high EA for $n=6, 13, 19, 23,$ and 29 atoms. High EA’s

suggest that the extra electron of the negative ion completes a shell; i.e., shell fillings are at 70 and 88 electrons, respectively. This disagrees with our finding of shell closings at $n_e = 68$ and 84 electrons.

Because a spherical approximation seems to be an appropriate starting point, we have considered symmetry-breaking perturbations which could explain the observed discrepancies: These include axially symmetric distortions (spheroidal or ellipsoidal), spin-orbit coupling, and crystal-field splitting. Based on twice the range of sizes as previous experiments, we find it impossible to fit our data by the ellipsoidally distorted shell model;^{4,13} the observed shell closings at $n_e = 50, 84, 114, 126,$ and 164 electrons are incompatible with this model. An estimate of the spin-orbit coupling constant in a cluster, following the calculations of Goepfert-Mayer,¹⁹ shows that this interaction is more than 1 order of magnitude too weak. The similarity of the pattern observed for Al and In, low- and high- Z atoms, would also appear to contradict this hypothesis.

Crystal-field effects in group-III clusters are more pronounced than in group-I metals because the $Z_A = 3$ ionic cores are larger perturbations on a jellium background. As in the case of the nearly-free-electron model of bulk metals, deviations from free-electron behavior occur when nodal surfaces in the electronic wave functions are commensurate with the ionic cores. Therefore, high- l shells in larger clusters will manifest this level splitting according to the structural symmetry of the cluster.¹¹ Conversely, the pattern of electronic levels can be used to infer information about structural symmetries. For example, the numerous gaps in the energy levels of an octahedral Al_{13} cluster²⁰ deviate considerably from the observed IP drops in clusters of similar size, lacking the observed major gaps at 20 and 40 electrons which are predicted by the spherical shell models. The energy-level pattern of McHenry *et al.*²¹ for icosahedral Al_{13} is, however, consistent with the observed IP drops. In I_h symmetry, $l=4$ (f) shells are the first to be split by symmetry lowering. Therefore, many of the energy gaps predicted by spherical models are retained, including those at $n_e = 20$ and 40 . In addition, a new gap not present in the SJBM is predicted at 50 electrons, in correspondence to the substantial IP drop at Al_{17} . While other structures (perhaps of low symmetry) cannot be ruled out in explaining the electronic structure of these clusters, the IP results presented here should motivate calculations on larger clusters of icosahedral symmetry. Furthermore, the importance of this structural motif is indicated by observations of icosahedral small metal particles²² and by the icosahedral symmetry (quasicrystals) in bulk Al-Mn alloy.²³

In conclusion, we have observed evidence for the hybridization of the s and p electronic bands in group-III metal atomic clusters. The onset is manifested in the abrupt leveling of IP’s near $n=5$ atoms and the hybridi-

zation is completed in the $n=25-45$ range after a gradual approach to the classical prediction. The size evolution IP's beyond $n=6$ exhibits an electronic shell structure qualitatively similar to that observed earlier in alkali metals. While many of the shell-filling numbers are those predicted by the spherical jellium model, other aspects of the electronic shell structure of the group-IIIA metal clusters are inconsistent, even for larger clusters. The most plausible explanation of the electronic level pattern is structural symmetry lowering from spherical symmetry resulting from lattice crystal-field effects. A full report on the photoionization spectroscopy of Al_n and In_n clusters is forthcoming.²⁴

We thank Professor M. Broyer for providing us with a preprint of their work (Ref. 9), and acknowledge helpful discussions with Dr. Tom Upton and Dr. Pierre Labastie. This work was supported by the Office of Naval Research and by the NSF. R.L.W. acknowledges support from the Sloan Foundation and the Packard Foundation.

Note added.—de Heer, Milani, and Châtelain²⁵ have recently measured the electric dipole polarizabilities of Al_n atomic clusters (n to 61) and interpreted the observed pattern in terms of a "nonjellium-to-jellium transition" occurring near 40 atoms. We find that the ionization potentials deviate significantly from the spherical model throughout the $n=30-60$ range, suggesting more complex behavior than a simple transition. The very low polarizabilities observed in the small cluster sizes could be due to a suppressed response of the deep s -band electrons, since this is the size region where s - p hybridization is occurring. In this case, the approach of IP's to the classical curve and the approach of the polarizabilities to the Thomas-Fermi jellium curve would be manifestations of the same effect.

^(a)Also at Department of Physics.

¹W. D. Knight *et al.*, Phys. Rev. Lett. **52**, 2141 (1984); W. A. Saunders, K. Clemenger, W. A. de Heer, and W. D. Knight, Phys. Rev. B **32**, 1366 (1985).

²For review, see W. A. de Heer, W. D. Knight, M. Y. Chou, and M. L. Cohen, in *Solid State Physics*, edited by H. Ehrenreich and D. Turnbull (Academic, New York, 1987), Vol. 40, p. 94.

³J. L. Martins, R. Car, and J. Buttet, Surf. Sci. **106**, 265 (1981); W. Ekardt, Phys. Rev. B **29**, 1558 (1984).

⁴K. Clemenger, Phys. Rev. B **32**, 1359 (1985).

⁵This model's success has been interpreted through finite-temperature computations on small sodium clusters which reveal weak correlation between ion and electron distributions; P. Ballone, W. Andreoni, R. Car, and M. Parrinello, Europhys. Lett. **8**, 73 (1989).

⁶M. Y. Chou and M. L. Cohen, Phys. Lett. **113A**, 420 (1986); D. E. Beck, Solid State Commun. **49**, 381 (1984).

⁷K. Rademann, B. Kaiser, U. Even, and F. Hensel, Phys. Rev. Lett. **59**, 2319 (1987); K. Rademann, Ber. Bunsenges. Phys. Chem. (to be published).

⁸C. Bréchnignac *et al.*, Phys. Rev. Lett. **60**, 275 (1988).

⁹D. Rayane *et al.*, Phys. Rev. A **39**, 6056 (1989).

¹⁰D. M. Wood, Phys. Rev. Lett. **46**, 749 (1981); C. Bréchnignac, Ph. Cahzac, F. Carlier, and J. Leygnier, Phys. Rev. Lett. **63**, 1368 (1989).

¹¹T. H. Upton, J. Chem. Phys. **86**, 7054 (1987); Phys. Rev. Lett. **56**, 2168 (1986); (unpublished).

¹²G. Ganteför, M. Gausa, K. H. Meiwes-Broer, and H. O. Lutz, Z. Phys. D **9**, 253 (1988).

¹³K. J. Taylor *et al.*, Chem. Phys. Lett. **152**, 347 (1988).

¹⁴D. M. Cox, D. J. Trevor, R. L. Whetten, and A. Kaldor, J. Phys. Chem. **92**, 421 (1988).

¹⁵M. F. Jarrold, J. E. Bower, and J. S. Kraus, J. Chem. Phys. **86**, 3876 (1987); W. Begemann *et al.*, Z. Phys. D **3**, 183 (1986).

¹⁶J. L. Persson and R. L. Whetten, Chem. Phys. Lett. **147**, 168 (1988); K. E. Schriver *et al.* (to be published).

¹⁷For discussion, see L. A. Turkevich and M. H. Cohen, Phys. Rev. Lett. **53**, 2323 (1984).

¹⁸The ordering given is that of Ekardt (Ref. 3) for Na. Slight changes in ordering may occur due to the increased electronic density of Al or the exact treatment of electron correlation and exchange (see Beck, Ref. 6), but major gaps between shells should occur at the same electron numbers.

¹⁹M. Goepfert-Mayer, Phys. Rev. **75**, 1969 (1949).

²⁰D. R. Salahub and R. P. Messmer, Phys. Rev. B **16**, 2526 (1977).

²¹M. E. McHenry, M. E. Eberhart, R. C. O'Handley, and K. H. Johnson, Phys. Rev. Lett. **56**, 81 (1986).

²²S. Iijima and T. Ichihashi, Phys. Rev. Lett. **60**, 2295 (1986).

²³D. Shechtman, I. Blech, D. Gratias, and J. W. Cahn, Phys. Rev. Lett. **53**, 1951 (1984).

²⁴J. L. Persson, K. E. Schriver, E. C. Honea, and R. L. Whetten (to be published).

²⁵W. A. de Heer, P. Milani, and A. Châtelain, Phys. Rev. Lett. **63**, 2834 (1989).

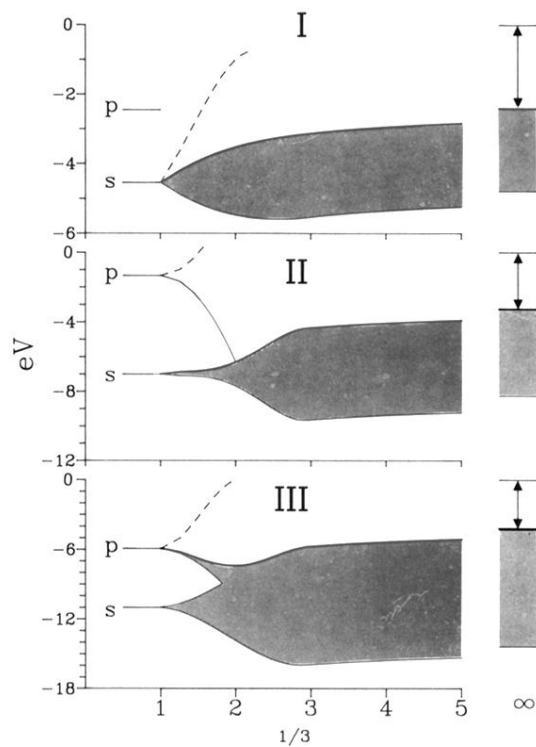


FIG. 2. Hypothetical size evolution of the electron bands of clusters composed of n group-I (upper), -II (middle), and -III (lower) metal atoms. The s and p orbital energies of the bulk Fermi energies and the work functions are defined with respect to vacuum and are appropriate to a mid- Z atom (e.g., Na or K, Mg or Ca, and Al or Ga). The asymptotic behavior of the work function is taken to be $n^{-1/3}$, as already observed for Na and K (Refs. 1 and 10) and in Fig. 1.